Performance Analysis of an Industrial Inkjet Printing Head Using the 1D Lumped Model

Won-Chul Sim[1], Sung-Jun Park[2,#] and Jaewoo Joung[1]

1 eMD Center, Central R&D Institute, Samsung Electro-Mechanics Co., Ltd., #314, Maetan-3-dong, YeongTong-gu, Suwon, Gyeonggi-do, South Korea, 443-743
2 Department of Mechanical Engineering, Chungju National University, 72 Daehak-ro, Chungju, Chungcheongbuk-do, South Korea, 380-702
Corresponding Author / E-mail: park@cjnu.ac.kr, TEL: +82-43-841-5130, FAX: +82-43-841-5120

KEYWORDS: Inkjet printing, Inkjet head, 1D lumped model, Direct writing

A design approach using a one-dimensional (1D) lumped model was studied and applied to an industrial inkjet printing head design for micro patterning on printed circuit boards. For an accurate analysis, a three-dimensional piezoelectric-driven actuator model was analyzed and its jetting characteristics were applied to 1Danalysis model. The performance of the 1D lumped model was verified by comparing measured and simulated results. The developed 1D model helped to optimize the design and configuration of the inkjet head and could be implemented in the design of multi-nozzle inkjet printing heads to improve the jetting frequency and minimize crosstalk.

Manuscript received: January 2, 2008 / Accepted: January 13, 2008

NOMENCLATURE

q	= flow rate
C	= compliance
M	= inertance
p	= pressure
R	= resistance
V	= volume change
V	= applied voltage

1. Introduction

Recently, inkjet printing methods have been examined with the aim of replacing conventional high-cost micro patterning processes on electronic devices, which include repeated mask masking, UV exposure, developing, chemical etching, resist stripping, cleaning, water rinsing, and drying.[1] With recent advances in the synthesis and stabilization of nano-sized particles in a specific medium, direct inkjet printing has become a promising solution for the deposition of materials in a wide variety of applications. Compared with conventional processes, inkjet printing technology has low costs, simpler processing, and a high rate of material utilization. The adoption of a reliable piezoelectric inkjet printing head is desirable for ejecting fine droplets, without variations in the droplet velocity and size. However, the absence of a reliable piezoelectric inkjet head for various functional inks prevents the application of inkjet printing technology during the manufacture of electronic products.[2] In this study, a bending-mode piezoelectric inkjet head was investigated for directly printing on printed circuit boards (PCBs) using liquid metal ink. A lumped element model was developed to predict the performance of the inkjet head for various head design parameters.

2. One Dimensional (1D) Lumped Model

A schematic view of the piezoelectric-driven drop-on-demand inkjet head is shown in Fig. 1. When an electric field is applied to a piezoelectric material, it changes its planar dimensions. If it is rigidly attached to the vibratory plate, bending occurs. This bending increases the pressure in a chamber and causes an ink droplet to be ejected through the nozzle. Demand ink jet heads are composed of a composite system of electrical, mechanical, and fluidic elements. However, the mathematical difficulty of predicting the performance of a printing head is greatly reduced by replacing the distributed components with equivalent lumped elements.[3-5] The displacement of a piezoelectric vibrator in a pressurization chamber and the resulting ink stream may be analogized to the electric circuit shown in Fig. 2, where C, M, and R illustrate the compliance, inertance, and resistance of the lumped elements, respectively. The fluid compressibility in the pressurization chamber is represented by C. The elastic deformation of the vibratory plate also acts as compliance. When accelerated ink flows through a thin passage, the mass of the ink acts as an inertance. In the notation, the subscript denotes the component of the inkjet head (*e.g.*, "p" for piezoelectric vibrator, "c" for pressure generating chamber, "r" for restrictor, "n" for nozzle, "*res*" for reservoir, and "m" for meniscus).

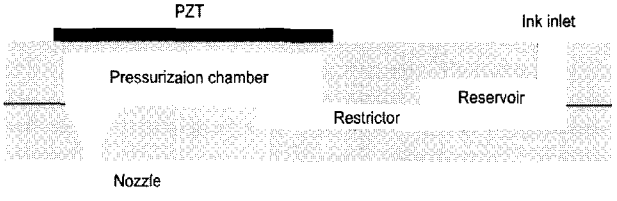

Fig. 1 Schematic diagram of the inkjet printing head

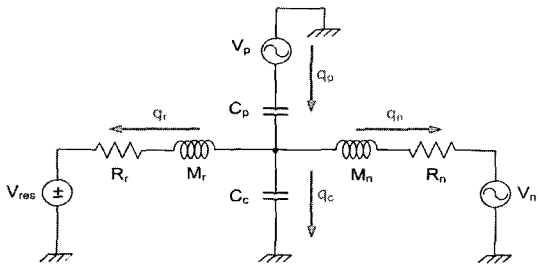

Fig. 2 Equivalent circuit diagram of the inkjet printing head

By using a lumped element model of the inkjet printing head, we obtain following equations.

$$\ddot{q}_r = -\frac{1}{M_r}\left\{R_r \dot{q}_r + \frac{1}{C_p + C_c} q_r + \frac{1}{C_p + C_c} q_n - \frac{C_p}{C_p + C_c} V_p + V_{res}\right\} \quad (1)$$

$$\ddot{q}_n = -\frac{1}{M_n}\left\{R_n \dot{q}_n + \frac{1}{C_p + C_c} q_r + \frac{1}{C_p + C_c} q_n - \frac{C_p}{C_p + C_c} V_p + V_m\right\} \quad (2)$$

Where $\ddot{q}_r$ and $\ddot{q}_n$ are flow rates at the restrictor and nozzle, respectively. Figure 3 shows a block diagram of the equivalent circuit for the inkjet printing head. Compared with the inertance and resistance of the nozzle and restrictor, M_c and R_c are sufficiently small that they can be neglected.

2.1 Piezoelectric Vibrator

An AC voltage V_p was applied across the piezoelectric vibrator to generate an effective pressure that drove the diaphragm into oscillation. Thus, a conversion ratio K_{eq} from the electrical domain to the fluidic domain with units of Pa/V must be considered.[6] K_{eq} can be calculated by comparing the displacement generated by the applied voltage and by the pressure. To obtain the compliance of the piezoelectric vibrator and K_{eq}, a finite element (FE) analysis was performed using the commercial FEM package CoventorWare. Figure 4 shows the simulated displacement contour of the piezoelectric vibrator used to acquire its compliance and the conversion ratio of the voltage to pressure:

$$C_p = \frac{V_a}{P} \quad (3)$$

$$K_{eq} = \frac{\left(\frac{v_V}{C_a}\right)}{V} \quad (4)$$

where V_a is the volume change due to the pressure, P is the applied pressure, v_V is the volume change due to the voltage, and V is the applied voltage.

2.2 Compliance

The fluid compressibility of the pressurization chamber acts as a compliance. The compliance of the pressurization chamber is given by

$$C_c = \frac{V_c}{\rho \alpha^2} \quad (5)$$

where V_c is the volume of the pressurization chamber, ρ is the density of the ink, and α is the speed of sound in the ink, which is approximately 1500 m/s.

2.3 Resistance

The pressure drop is caused by viscous losses in the inkjet channels. In addition, when fluid moves through the flow passages, a sudden change of the cross-sectional area occurs between both

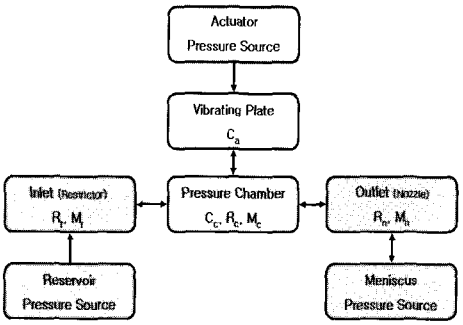

Fig. 3 Block diagram of the one-dimensional lumped model used for the analysis of inkjet head

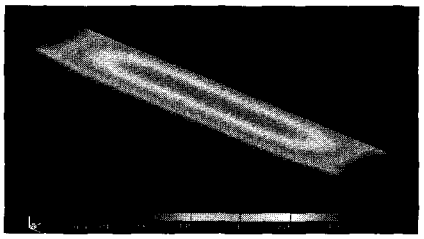

Fig. 4 Simulated displacement corresponding to an applied voltage for calculating the compliance of the vibrator and K_{VtoP} in the lumped element analysis

the pressurization chamber and the restrictor and nozzle, as shown in Fig. 5. Thus, the effect of the sudden expansion and contraction must be considered when calculating the pressure drop:

$$\Delta P = R\dot{q} + R_{se}\dot{q}^2 + R_{sc}\dot{q}^2 \quad (6)$$

where $\dot{q}$ is the flow rate and R_{se} and R_{sc} are the resistances at the sudden expansion and contraction. Based on Eq. (4),

$$\Delta P_{res} = R_r \dot{q}_i + R_{se}\dot{q}_i^2 + R_{sc}\dot{q}_i^2 \quad (7)$$

$$\Delta P_{noz\_in} = R_n \dot{q}_o + R_{se}\dot{q}_o^2 \quad (8)$$

$$\Delta P_{noz\_out} = R_n \dot{q}_o + R_{sc}\dot{q}_o^2 \quad (9)$$

where R_r and R_n are

$$R_r = 128\mu\frac{L_r}{D_{eff\_r}^2} \quad (10)$$

$$R_n = 128\mu\frac{L_r}{\pi \cdot D_n^2} \quad (11)$$

Here, L_r is the length of the restrictor, L_n is the length of the nozzle, μ is the ink viscosity, D_{eff_r} is the effective diameter of the restrictor, and D_n is the nozzle diameter. The resistance due to the change of the cross-section is given by

$$R_{se} = \frac{\rho k_{se}}{(2 \times A^2)} \tag{12}$$

$$R_{sc} = \frac{\rho k_{sc}}{(2 \times A^2)} \tag{13}$$

where A is the cross-sectional area of the sudden expansion and contraction, K_{se} is the loss coefficient of the sudden expansion, and K_{sc} is the loss coefficient of the sudden contraction, which are empirically determined.

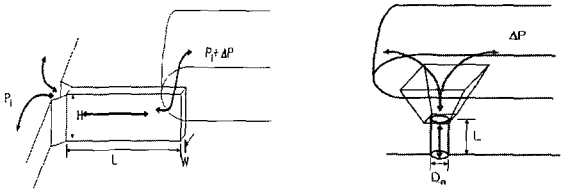

(a) from restrictor to chamber (b) from chamber to nozzle

Fig. 5 Flow in the (a) restrictor and (b) nozzle

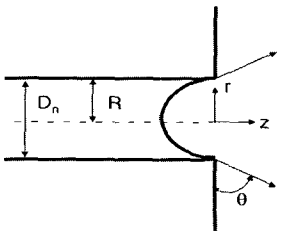

Fig. 6 A simplified shape of the meniscus in a circular orifice

2.4 Inertance

When ink flows through a thin passage, the inertia of the ink is represented by the inertance. The inertance is given by

$$M = \beta \cdot \rho \frac{L}{A} \tag{14}$$

where β is an empirical coefficient and A is the cross-section area.

2.5 Meniscus

The pressure generated by deflecting an elastic vibrator is balanced with the action of the fluid surface tension in the orifice. To estimate the pressure of a meniscus with a circular cross-section, we assume that the profile of the meniscus maintains a parabolic shape, as shown in Fig. 6:

$$z = Z_{\max}\left(1 - \frac{r^2}{R^2}\right) \tag{15}$$

The pressure change driven by the equilibrium condition between the surface tension and the generating pressure is

$$\Delta P = \frac{4\sigma}{D_n}\sqrt{\frac{16 \cdot Z_{\max}^2}{16 \cdot Z_{\max}^2 + D_n^2}} \tag{16}$$

where Z_{max} is the maximum displacement of the meniscus, R is the nozzle radius, and σ is the surface tension.

3. 1D Lumped Analysis

3.1 Numerical Analysis

The one-dimensional lumped model solutions were obtained numerically using a fourth-order Runge-Kutta integration algorithm to solve the differential equations. A flow chart of the program is shown in Fig. 7.

3.2 Verification of the 1D Model

The performance of the model was evaluated when the voltage waveform depicted in Fig. 8 was applied. The waveform consisted of five parts: 1.5 μs of falling (t_1), 6.5 μs of holding (t_2), 1.5 μs of rising (t_3), 14.5 μs of holding (t_4), and 1.5 μs of falling (t_5). The operating driving voltage ranged from -15 to +40 V. The viscosity and surface tension of the ink were 4.8 cPs and 0.025 N/m, respectively. The simulated and measured results are compared in Table 1 Both the predicted droplet velocity and drop volume matched well with the experimental results.

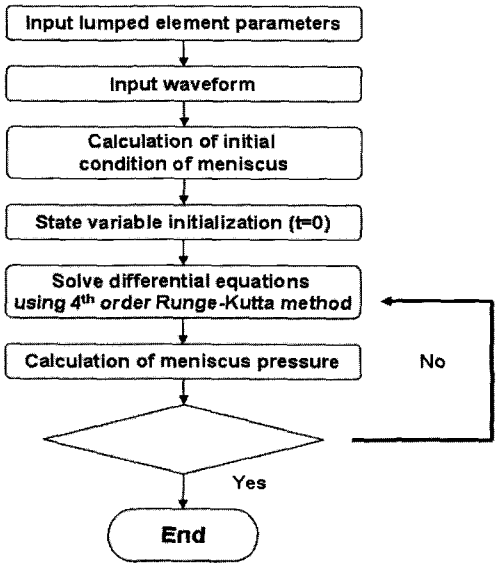

Fig. 7 Flow chart of the 1D analysis program

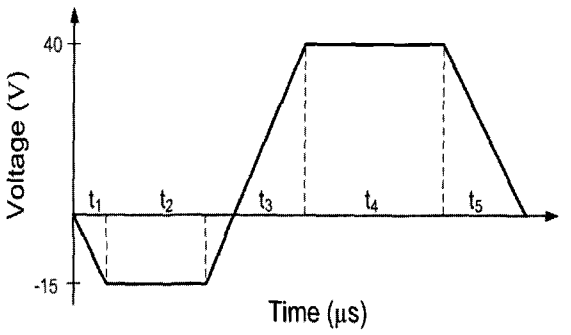

Fig. 8 Waveform of the driving voltage signal applied to the inkjet head

Table 1 Comparison between simulated and measured results

	1D analysis (predicted)	Experiment (measured)	Error (%)
Droplet volume [pl]	24.2	27.5	12
Jetting velocity [m/s]	3.6	3.8	6

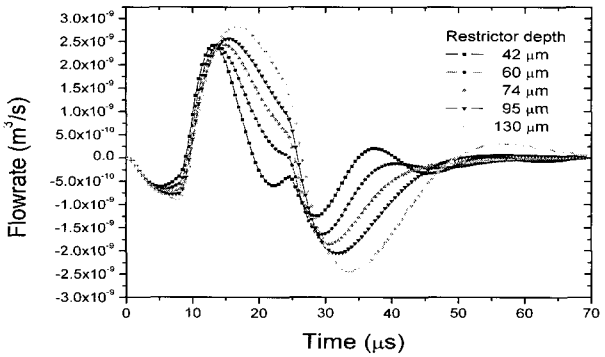

Fig. 9 Flow rate at the nozzle for various restrictor depths

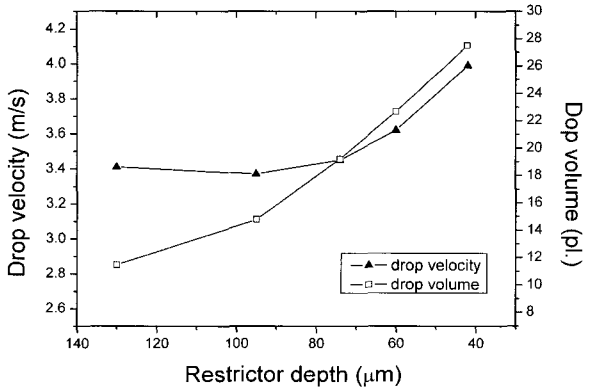

Fig. 10 Droplet volume and velocity for various restrictor depths

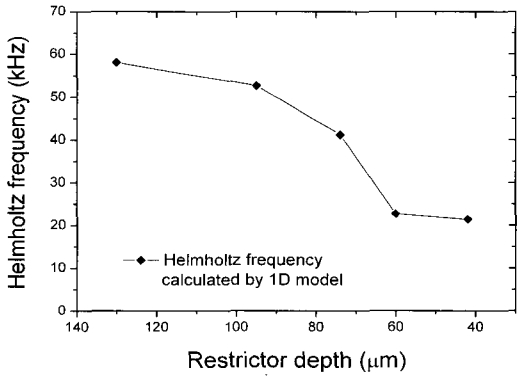

Fig. 11 Helmholtz resonance frequency for various restrictor depths

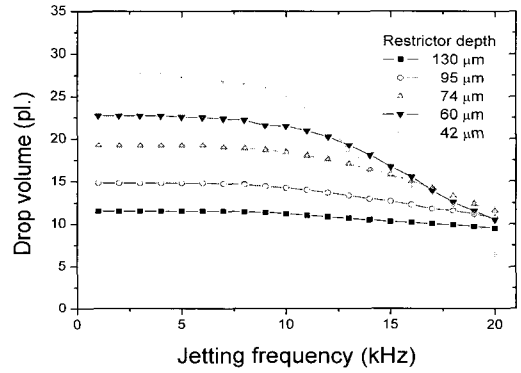

Fig. 12 Droplet volume for various jetting frequencies

4. Results: Jetting Performance

Using the one-dimensional lumped analysis, we characterized the flow rate at the nozzle for various restrictor depths, as shown in Fig. 9. Since a decrease in the restrictor depth caused the flow resistance at the restrictor to increase, the fluid moving into the nozzle also increased. Therefore, as depicted in Fig. 10, the droplet volume increased with the restrictor depth. The Helmholtz resonance frequency of the inkjet printing head decreased with the reduction of the restrictor depth, as shown in Fig. 11. This phenomenon influenced the characteristics of the inkjet head jetting frequency. Figure 12 shows the droplet volume for various jetting frequencies up to 20 kHz. At a restrictor depth of 130 μm, the droplet volume did not change with variations in the ejection frequency. However, at a restrictor depth of 42 μm, the droplet volume dramatically changed with variations in the jetting frequency due to insufficient ink supply.

5. Conclusions

Simplified one-dimensional lumped modeling approach was developed and applied to the design of an industrial inkjet head. The configuration of the inkjet printing head was simplified to the equivalent electric circuit using lumped elements, which were acquired theoretically from the governing equations. The results demonstrated that the one-dimensional lumped analysis accurately evaluated the performance of the designed inkjet printing head. They also helped us to understand the effect of the driving voltage waveform on the increase in the droplet velocity and the reduction of the droplet size, which is important for directly writing on printed circuit boards. Our modeling approach can be used as a tool to improve the design of piezoelectric inkjet printing heads, resulting in better jetting performance.

REFERENCES

1. Legierse, P. E. J., "Inkjet Printing in the Electronics Industry," Digital Production Printing and Industrial Applications: Eye on the Future, Vol. 1, pp. 197-200, 2001.
2. Stephen, F., "Inkjet Technology and Product Development Strategies," Torrey Pines Research, pp. 198-201, 2000.
3. Kyser, E. L., Collins, L. F. and Herbert, N., "Design of an Impulse Inkjet," Journal of Applied Photographic Engineering, Vol. 7, No. 3, pp. 73-79, 1981.
4. Kyser, E. L. and Sears, S. B., "Method and Apparatus for Recording with Writing Fluids and Drop Projection Means therefore," U.S. Patent, No. 3946398, Siliconics Inc., 1976.
5. Sim, W., Park, S-J., Park, C., Kim, C. S., Yoo, Y., Yang, C., Kim S., Kim, Y., Yang, J., Joung, J. and Oh, Y., "Analysis of the Droplet Ejection for Piezoelectric-driven Industrial Inkjet Head," NSTI-Nanotech, Vol. 2, pp. 528-533, 2006.